Origin and transportation history of lunar breccia 14311

Renaud E. MERLE [1,2], Alexander A. NEMCHIN[1], Martin J. WHITEHOUSE[3], Robert T. PIDGEON[1], Marion L. GRANGE [1], Joshua F. SNAPE[3] and Fiona THIESSEN[3].

Affiliations:

1: Department of Applied Geology, Curtin University, GPO Box U1987, Perth, WA 6845, Australia

2: Australian National University, Research School of Earth Sciences, 142 Mills Rd, Acton, ACT 0200, Australia.

3: Department of Geosciences, Swedish Museum of Natural History, S-104 05, Stockholm Sweden.

* Corresponding author: renaud.merle@anu.edu.au

ABSTRACT

In this paper we compare the U-Pb zircon age distribution pattern of sample 14311 from the Apollo 14 landing site with those from other breccias collected at the same landing site. Zircons in breccia 14311 show major age peaks at 4340 Ma and 4240 Ma and small peaks at 4110 Ma, 4030 Ma and 3960 Ma. The zircon age patterns of breccia 14311 and other Apollo 14 breccias are statistically different suggesting a separate provenance and transportation history for these breccias. This interpretation is supported by different U-Pb Ca-phosphate and exposure ages for breccia 14311 (Ca-phosphate age: 3938 ± 4 Ma, exposure age: ~550-660 Ma) from the other Apollo 14 breccias (Ca-phosphate age: 3927 ± 2 Ma, compatible with the Imbrium impact, exposure age: ~25-30 Ma). Based on these observations, we consider two hypotheses for the origin and transportation history of sample 14311:

(1) Breccia 14311 was formed in the Procellarum KREEP terrane by a 3938 Ma-old impact and deposited near the future site of the Imbrium basin. The breccia was integrated into the Fra Mauro Formation during the deposition of the Imbrium impact ejecta at 3927 Ma. The zircons were annealed by mare basalt flooding at 3400 Ma at Apollo 14 landing site. Eventually, at approximately 660 Ma, a small and local impact event excavated this sample and it has been at the surface of the Moon since this time.

(2) Breccia 14311 was formed by a 3938 Ma-old impact. The location of the sample is not known at that time but at 3400 Ma it was located nearby or buried by hot basaltic flows. It was transported from where it was deposited to the Apollo 14 landing site by an impact at approximately 660 Ma, possibly related to the formation of the Copernicus crater and has remained at the surface of the Moon since this event.

This latter hypothesis is the simplest scenario for the formation and transportation history of the 14311 breccia.

INTRODUCTION

Lunar zircons in impact breccias show complex age distribution patterns that carry information about the early magmatic and impact history of the Moon (e.g. Nemchin et al. 2008; Taylor et al. 2009; Hopkins and Mojzsis 2015). These patterns also provide information on zircon provenance and the history of the target material from which the breccias were formed. A comparison of age distribution patterns obtained from different breccia samples gives additional information linking these samples to the formation of specific impact craters (basins). For example, the zircon age patterns can provide constraints on the age of the Imbrium basin forming and the origin of rocks collected at the Apollo 14 landing site that are believed to belong to its ejecta (the material excavated from the cavity created by the Imbrium impact event). Previous age estimates for the Imbrium impact range from 3770 to 3920 Ma (Deutsch and Stöffler 1987; Stadermann et al. 1991; Dalrymple and Ryder 1993; Shih et al. 1993; Gnos et al. 2004; Liu et al. 2012), with the latter being used recently as the preferred age for this impact (Gnos et al. 2004; Liu et al. 2012). This older limit is in agreement with the $^{207}Pb/^{206}Pb$ age of 3927 ± 2 Ma (2σ) obtained from Ca-phosphate grains from three Apollo 14 impact breccias (14305, 14306 and 14314) and also interpreted as the age of the Imbrium impact event (Snape et al. 2016). It is significantly younger than the $^{207}Pb/^{206}Pb$ age of 3938 ± 4 Ma (2σ) yielded by Ca-phosphates from breccia 14311

(Merle et al. 2014), which as a result was interpreted as representing an impact that pre-dates formation of the Imbrium basin, possibly the Humorum or Serenitatis impact (Snape et al. 2016). It should be noted that errors determined for the phosphate ages by both Snape et al. (2016) and Merle et al. (2014) do not include uncertainties in the U decay constants. These uncertainties would introduce a systematic error component to the defined ages. While this can increase errors of individual ages to about 8 Ma (2σ), it has very little influence on the difference between two ages (less than 15 Kyr uncertainty at 2-sigma level when comparing two dates in the 3.9 Ga range). Consequently uncertainties in U decay constants make a negligible contribution and can be ignored when comparing two ages determined using the U-Pb isotope system. Uncertainties on decay constants have to be taken into account when ages are determined using different chronometers such as U-Pb and ^{39}Ar-^{40}Ar systems (e.g. Schoene et al., 2006).

In this contribution new zircon U-Pb ages from breccia 14311 are presented. This sample was selected as it presents significant textural and petrological differences, an older exposure age (550-660 Ma, Drozd et al. 1974; Stadermann et al. 1991) and an older Ca-phosphate age 3938 ± 4 Ma (Merle et al. 2014) compared to the other breccia samples collected at the Apollo 14 landing site (exposure age: ~ 30 Ma, Stadermann et al. 1991; Ca-phosphate age: 3927 ± 2 Ma, Snape et al., 2016). These findings led several authors to interpret it as originating from a separate impact event (e.g. Stöffler et al. 1989; Stöffler 1989; Stadermann et al. 1991). This new dataset is compared with previously published zircon ages for this sample and other breccia samples in order to further investigate differences between 14311 and other breccias collected at the Apollo 14 site.

SAMPLE 14311 IN THE CONTEXT OF APOLLO 14 LANDING SITE

The Apollo 14 landing site is located 600-800 km from the rim of the ~ 3900 Ma Imbrium basin (Fig. 1). Pre-mission mapping and early studies of images of the lunar surface indicated that the region at and around the Apollo 14 landing site is covered by ejecta from the Imbrium impact, named the Fra Mauro Formation (e.g. Swann et al. 1977). The landing site was selected for its proximity to the ~ 30 Ma Cone Crater (Fig. 1) that is thought to have penetrated through the surface regolith and excavated rocks of the Fra Mauro Formation (Swann et al. 1977), hence giving the opportunity to investigate the deposits of one of the largest impacts on the Moon. The landing site can be subdivided into the Cone Crater ejecta and a smooth, older terrane around the site (Stöffler et al. 1989), which is formed mostly by regolith and regolith breccias. Two types of impact breccias have been identified. In the vicinity of Cone Crater, friable light matrix breccias (Meyer 2008) are the dominant type and supposedly form its continuous ejecta blanket. Further away, crystalline-matrix breccias (Meyer 2008) are very abundant and possibly represent the discontinuous ejecta blanket of the Cone Crater impact event (Wilshire and Jackson 1972; Stöffler et al. 1989).

Wilshire and Jackson (1972) argued that since the major ridge structure of the Fra Mauro Formation is not disturbed significantly by later impacts, both the light matrix and the crystalline-matrix breccia types originate from the same impact and are related to the formation of the Imbrium basin. Therefore, the Fra Mauro Formation represents a heterogeneous ejecta blanket from the Imbrium impact. This interpretation is also supported by Swann et al. (1977), who suggested that only the upper third of the Fra Mauro Formation was penetrated by the Cone Crater impact, assuming an estimated thickness of the formation of 100-200 m (Eggleton and Offield 1970). However, the thickness of the Fra Mauro Formation is not well constrained and estimates vary between 150 and 35 m (Eggleton and Offield 1970; Kovach et al. 1971; McGetchin et al. 1973). Moreover, the variable degree of re-equilibration displayed by Apollo 14 breccia matrices is interpreted to reflect a relatively slow differential cooling in a single impact ejecta blanket (Warner 1972; Williams 1972). Temperature estimates based on this model suggest heating of most equilibrated breccias to about 1100-1300^{o}C (e.g. Williams 1972; Lindsay 1975). Finally, all the collected samples are typically rich in KREEP (lunar mantle component enriched in K, REE and P) and their chemical similarity was also used to argue for formation in a single impact event (Jolliff et al. 1991; Korotev et al. 2011).

A different view was expressed in a series of papers by Stöffler and co-workers (e.g. Stöffler et al. 1989; Stöffler 1989; Staderman et al. 1991 and reference therein) based on both of both textural features observed in the Apollo 14 breccias and the distribution of different impact breccia types relative to the Cone Crater. They proposed that only the crystalline-matrix breccias, mostly collected further from Cone Crater, are representative of the Imbrium event. These breccias are suggested to originate from a layer immediately underneath the surface regolith and named the "subregolith basement" (Stöffler 1989). The light-matrix breccias collected near Cone

Crater may represent a deeper stratigraphic unit named the "Cone Crater basement" that predates the Imbrium impact (Stöffler 1989). If this hypothesis is correct, it implies that old material, potentially originating from a Nectarian or pre-Nectarian impact, was reworked at the time of Fra Mauro Formation deposition (Stöffler et al. 1989).

There is a general agreement that at least part of the sampled material represents genuine Imbrium ejecta. Nevertheless, at the time of its deposition, this ejecta could also have been mixed with older local material at the landing site (Hawke and Head 1978; Stöffler 1989). For example, Haskin et al. (2002) proposed that the Fra Mauro Formation consists of 58% Imbrium ejecta, whereas Morrison and Oberbeck (1975) suggested that this formation is mainly formed by local impact ejecta with only 15 to 20% Imbrium ejecta.

This division into "Cone Crater basement" and "subregolith basement breccia" seems to be supported by a difference in exposure ages of the samples collected across the entire landing site. Indeed, both crystalline-matrix breccias and light-matrix breccias occurring in the inferred Cone Crater ejecta yielded exposure ages compatible with the Cone Crater impact (at ~30 Ma) while crystalline-matrix breccia samples collected outside the Cone Crater ejecta have significantly older exposure ages (>100 Ma, Drozd et al. 1974; Stadermann et al. 1991).

STUDIED SAMPLE

Sample 14311 was collected close to a small crater at Station Dg (Fig. 1). It is a very coherent polymict impact-melt breccia composed of 75 to 95% crystalline-matrix formed by a mosaic of pyroxene and plagioclase crystals or crystal fragments and Fe-Ti oxides (Fig. 2), the remaining 5 to 25% consisting of mineral and lithic clasts, represented by igneous rocks and older generations of breccias (Simonds et al. 1977; Swann et al. 1977; Carlson and Walton 1978). Rare olivine clasts formed reaction coronas with the impact melt (Wilshire and Jackson,1972). The mineralogy of the coronas varies according to the composition of olivine and includes pigeonite, ilmenite, orthopyroxene and plagioclase (Cameron and Fisher, 1975). Accessory minerals in the breccia 14311 include zircons and Ca-phosphates (Fig. 2).

While this sample is chemically similar to other impact breccias from this landing site (Scoon 1972), it is the only crystalline-matrix breccia collected near Cone Crater and has older cosmic-ray exposure age estimates (based on noble gas clocks at ~550-660 Ma, Stadermann et al. 1991; Drozd et al. 1974). As a consequence, Stöffler and co-workers (e.g., Stöffler et al. 1989; Stöffler 1989; Stadermann et al. 1991) suggested that it might originate from a different part of the Fra Mauro Formation.

Early Secondary Ion Mass Spectrometry (SIMS) U-Pb measurements yielded an age of 4250 ± 4 (2σ) Ma for a large euhedral zircon from section 14311,90 (Meyer et al. 1996) which was interpreted as dating pre-breccia source rocks that have been thoroughly mixed in the breccia. From an extensive SIMS study of the U-Pb systems of 112 zircons from breccia 14311, Hopkins and Mojzsis (2015) showed that zircon ages fall into at least three distinct populations at 4334 ± 10 Ma (2σ), 4245 ± 10 Ma and 3953 ± 10 Ma. Based on U-Pb concordance, REE patterns, igneous Th/U ratios and igneous zoning structures, Hopkins and Mojzsis (2015) interpreted the zircons as mineral fragments predating the formation of the breccia. These authors reported that this pattern of ages was similar to that observed in zircons from other breccias from Apollo 14 (Nemchin et al. 2008). Ca-phosphate grains present in this sample were dated using the U-Pb SHRIMP (Sensitive High Resolution Ion Microprobe) technique and yielded a $^{207}Pb/^{206}Pb$ age of 3938 ± 4 Ma (Merle et al. 2014). This is interpreted as the age of the breccia formation and represents a pre-Imbrium impact age. Zircons from 14311 analysed by Raman spectroscopy yielded an average model age (annealing age) of 3410 Ma ± 80 Ma (2σ), interpreted as a mild thermal event possibly represented by mare basalt eruption (Pidgeon et al. 2016). This thermal event was hot enough to anneal the radiation damage in the zircons (~ 230 °C) but still below the U-Pb system closing temperature of the Ca-phosphates (450–500 °C; Cherniak et al. 1991; Krogstad and Walker 1994; Chamberlain and Bowring 2000).

ANALYTICAL PROCEDURES

U-Pb systematics of zircons from five thin sections of the impact-melt breccia 14311 (14311,4; 14311,5; 14311,7; 14311,8 and 14311,90) have been investigated by SIMS. Polished thin sections of breccia samples were prepared at NASA's Johnson Space Centre. All the samples were gold coated prior to investigation of zircon internal micro-structures by scanning electron microscope and SIMS U-Pb isotope analyses.

Zircon grains were identified in the thin sections using an optical microscope and their presence was confirmed using an EDS (Energy Dispersive X-Ray Spectroscopy) system attached to a Zeiss EVO scanning electron microscope at Curtin University. The acceleration voltage applied during several sessions was set between 15 and 20 kV and the working distance at 8.5 mm. Prior to SIMS analysis, cathodoluminescence (CL) images of all zircon grains were obtained to characterize possible internal structures, using a Philips XL 30 scanning electron microscope at Curtin University. The acceleration voltage applied during several CL imaging sessions was set at 12 kV and the working distance at approximately 15 mm.

U-Pb analyses of zircon in thin sections 14311,4, 14311,8 and ten grains from thin section 14311,5 were performed at the NordSIMS facility using a high resolution CAMECA IMS1280 instrument following analytical protocol described elsewhere (Whitehouse et al. 1999; Whitehouse and Kamber 2005). A summary of analytical procedures is as follows: oxygen beam (O_2^-) at -13 kV was imaged through an aperture, giving a current ranging from 0.8 to 1 nA in an elliptical, approximately 7 µm spot. Secondary ions were extracted from the sample at +10 kV and admitted, via high magnification transfer optics, to the mass spectrometer operating at a mass resolution (M/ΔM) of 5400. Oxygen flooding of the sample chamber was used to enhance Pb^+ yield. At the start of each analysis, a 2 minute pre-sputter raster over a square of 15x15 µm was used to remove the Au coating and minimize surface contamination. This was followed by automated centering of the beam in the field aperture, optimisation of mass calibration of secondary ion energy in the 45 eV energy window, all using the $^{90}Zr_2{}^{16}O$ peak at nominal mass 196. The peak-hopping data collection routine consisted of 16 cycles through the defined mass stations, with signals measured on an ion counting electron multiplier with a 44 ns electronically gated dead time. Pb/U ratios were calibrated using an empirical correlation between Pb^+/U^+ and UO_2^+/U^+ ratios, normalised to the 1065 Ma Geostandards 91500 zircon (Wiedenbeck et al., 2004).

U-Pb analyses of zircon in thin section 14311, 90, 14311,7 and five grains from thin section 14311,5 were obtained on a SHRIMP II instrument at Curtin University. The analytical conditions were identical to those described by Compston et al. (1984) and Williams (1998). The samples were analysed with the intensity of the O_2^- primary beam set between 1.1 and 2.3 nA and an elliptical spot of 20 µm. Pb/U and Pb/Th calibration was made relative to the 562 Ma CZ3 zircon standard (Pidgeon et al. 1994), which was analysed after every five unknowns throughout the analytical sessions. The raw data were reduced using the Squid 2 algorithm (Ludwig 2009). Common Pb was corrected using the present-day terrestrial ratios from Stacey and Kramers (1975) assuming that all common Pb is surface contamination during sample preparation.

All the analytical results are given in Table 1. Data were plotted on a Tera-Wasserburg Concordia diagram using the Excel add-in Isoplot3 (Ludwig, 2008). The uncertainties of all the ages are $^{207}Pb/^{206}Pb$ ages discussed in the following section are given at 2 sigma level.

RESULTS

The analysed zircons from 14311 thin sections (14311,4; 14311,5; 14311,7, 14311,8 and 14311,90) occur as separate crystals and fragments scattered in the breccia matrix. Crystals are usually smaller than 100 µm in length and have sharp contacts with the matrix (Fig. 2a, b and c). Euhedral grains are very rare in the analysed population, the majority of zircons being preserved as fragments showing variable external morphology ranging from angular to smooth or rounded (Fig. 2a, b and c). Radial fractures are observed in the matrix around some grains (Fig. 2d) and are attributed to an increase in volume of the zircon grain resulting from in situ radiation damage. None of the analysed grains show any textural evidence of crystallisation from the impact melt that consolidated the sample. Consequently, they are all interpreted as crystals or fragments predating breccia formation. Their shapes suggest that they were fragmented and abraded during the impact and the subsequent transport and deposition of the ejecta blanket. Most of the grains show very low intensity in CL signals.

Grains larger than 50x20 µm were suitable for multi-spot SIMS analysis while grains smaller than 10x10 µm were not analysed. A total of seventy-five analyses were made on fifty-one grains (Table 1). Forty zircons were relatively small, allowing only one spot to be analysed on their surface. Eleven grains were large enough to place several (2 to 6) analytical spots. For each of these grains, these multiple spots yielded identical ages within uncertainties and the ages of the grains were defined by calculating the weighted average $^{207}Pb/^{206}Pb$ ages using all analysed spots.

All data are concordant to slightly discordant on the Concordia diagram (Fig. 3) forming two dense populations, one older than 4300 Ma and the other between 4300 Ma and 4200 Ma while a third less dense population of data gives ages between about 4150 and 3950 Ma (Table 1, Fig. 3). Note that the youngest zircon analysed in 14311 yielded an age of 3932 ± 23 Ma that is similar within uncertainties to the youngest zircon analysed in the previously published 14311 zircon ages dataset (3937 ± 18 Ma;

Hopkins and Mojzsis 2015) and the Ca-phosphate age of 3938 ± 4 Ma (Merle et al. 2014).

DISCUSSION

Comparison of zircon ages dataset from Apollo 14 breccias

The substantial number of individual zircon ages published from the sample 14311 by Hopkins and Mojzsis (2015) combined with the data presented here permits assessment of how representative the samples are and data reproducibility based on the results obtained independently in two different laboratories. It also allows comparison of the zircon age distribution pattern in 14311 and other Apollo 14 breccias. While the latter combines zircon grains from several samples that do not necessarily have the same provenance, such a comparison can still provide valuable information related to the homogeneity of zircon populations across the Apollo 14 landing site.

Prior to the comparison of zircon age distribution patterns in breccia samples, previously published data have been recalculated using an approach similar to that adopted for our data from sample 14311, i.e., a single analysis was taken as the age of a grain from which only one analysis was made, while a weighted average $^{207}Pb/^{206}Pb$ ages were adopted for grains from which multiple, statistically indistinguishable analyses are available.

Statistical methods designed to compare probability density plots (PDPs) of zircon ages are extensively developed for the assessment of provenance of detrital zircon populations in the sedimentary rocks on Earth. Several approaches have been proposed during the last 20 years (e.g. Sambridge and Compston, 1994; Gehrels, 2000; Sircombe and Hazelton, 2004; Sircombe, 2000; Fedo et al., 2003; Vermeesch, 2013; Satkoski et al., 2013), although none of these methods provides a completely unambiguous way to determine whether two distributions are similar or different. A significant pitfall of many is that they usually define parameters representing per cent of similarity/overlap between two PDPs, but do not determine a limiting value at which two distributions can be considered similar or different. For example applying the “likeness” parameter suggested by Satkoski et al (2013) for comparison of 14311 zircon data presented here and those published by Hopkins and Mojzsis (2015) results in the “likeness” of 79% (values approaching 100% in this approach represent high degree of a “likeness” between two distributions). When comparing all 14311 data, combined, with the zircon ages of all other Apollo 14 breccias (from Nemchin et al. 2008 and Taylor et al. 2009) the calculated degree of “likeness” is 69%. Both values are high suggesting the presence of some similar groups of zircon present in all Apollo 14 samples, but the ultimate decision about the variability of Apollo 14 zircon population is still subjective and does not provide confidence exceeding that obtained from the simple visual examination of PDPs.

Some of the more traditional statistical approaches like Kolmogorov-Smirnov test (KS-test), while not entirely problem free, may provide a more reliable way to compare two age distributions. The test is designed to compare distributions of two samples without making any assumption about the distribution of data and aims to determine if statistical difference exists between two populations. In the context of zircon age distribution patterns, the probability calculated by the K-S test represents the probability that two populations could have been selected randomly from the same parent population. If the p-value generated as a part of K-S test is high (typically above 0.05, at 95% level of confidence), it is unlikely that two samples are from two different populations.

Comparison of our new dataset to those of Hopkins and Mojzsis (2015) using the KS-test yields P of 0.35, indicating that the zircons from our study and from Hopkins and Mojzis (2015) can be drawn from the same population. As a consequence, we combined the two datasets from the 14311 breccia and compared it with the data from the other Apollo 14 landing site breccias (breccia samples 14066, 14303, 14304, 14305, 14306 and 14083) investigated by Nemchin et al. (2008 and Taylor et al. (2009). When comparing the combined 14311 dataset with the other breccias, the K-S test yielded P value of 0.04. As a consequence, we infer that breccia 14311 is different from the other breccias collected on the Apollo 14 landing site, i.e. at least some zircon groups present in 14311 are not found in the rest of the samples and vice versa.

Zircon age distribution and source of Apollo 14 breccias

The distribution of the detrital zircon ages over time has been represented using Kernel Density estimates (KDE) using the algorithm proposed by Vermeesch, (2012), rather than more traditional probability density plots (e.g. Ludwig, 2003; Sircombe, 2004). The latter is biased towards the high precision analyses and in some cases when the number of analyses and their precision is high can produce counter intuitive results

(Vermeesch, 2012). In contrast KDE is based on the density of available measurements and helps to avoid problems associated with the probability density plots. KDE is constructed using $^{206}Pb/^{207}Pb$ ages by arranging the measurements along a line and stacking a so-called "kernel" (in this case, a Gaussian curve) of a given width named "bandwidth" (Vermeesch, 2012). We adopted an adaptive kernel density estimation in which the bandwidth varies according to the local density of data. Such an approach is more appropriate in the case of age distributions that are not unimodal and smooth. In areas where data density is sparse, a large bandwidth is used, and the distribution is smoothed. Where lots of data are available, a narrower bandwidth is used allowing the KDE to provide a higher resolution estimate in those parts of the distribution. Since the relative errors generally show less grain-to-grain variability than the absolute errors, we applied a logarithmic transformation of the data (Galbraith, 1990) as recommended by Vermeesch (2012).

The most pronounced difference between sample 14311 and other Apollo 14 breccias can be resolved using a probability density plot (Fig. 4) and is observed in the time interval between 4.30 and 4.15 Ga. Sample 14311 has an age peak at about 4240 Ma in comparison to the other breccias defining an age distribution peak at about 4200 Ma. These age peaks correspond to a large proportion of the total data sets and do not overlap (Fig. 4) suggesting a real difference between the distributions. A significant difference in age distributions is also highlighted by the observation that two thirds of the zircon grains in the 4.30 and 4.15 Ga time interval from 14311 are older and two thirds of the grains investigated in other Apollo 14 breccias are younger than 4230 Ma (Table 1).

In addition, younger ages in 14311 are distributed equally between three minor peaks at approximately 4110 Ma, 4030 Ma and 3960 Ma, whereas the distribution of ages for all other Apollo 14 breccias is centred at approximately 4020 Ma. Nevertheless, the significance of these small peaks as true events and consequently the potential difference between the samples are difficult to assess due to the relatively small number of younger zircon grains present/analysed in this part of the age spectrum of the Apollo 14 samples.

The Moon has experienced a long history of magmatic and impact events and the observed zircon ages are likely to reflect this complexity of lunar evolution. Distinguishing magmatic from impact related zircon grains, however, is not trivial. Several features such as amorphisation and partial recrystallisation observed in the studies of some lunar zircon grains have been used as evidence that parts of these grains were affected by impacts (Pidgeon et al., 2007; Grange et al., 2013). Similarly, other internal structures such as granular domains and planar deformation features that are commonly observed in terrestrial impact structures (e.g. Cavosie, 2015), are sometimes also present in lunar zircon (Grange et al., 2013). Nevertheless, datable internal features in zircon can be only recognised as impact related in grains that also preserve original magmatic areas, in such cases providing an opportunity to obtain both the original magmatic age and the time of impact. A significant number of lunar zircon grains preserved in breccia samples are fragments that may represent disintegrated original crystals that recorded both magmatic and impact events, but when these crystals are fragmented the ability to distinguish impact related from magmatic parts is lost.

Liu et al. (2012) and Gnos et al. (2004), studying textural relationships of zircon and rock forming minerals in Apollo 12 samples as well as lunar meteorite SaU 169, recognised that some lunar zircon grains can form directly in an impact melt. Nevertheless, if such grains are removed from their original mineral assemblage as a result of a subsequent impact event and transferred into a breccia matrix, their impact related origin is also impossible to establish.

Hopkins and Mojzsis (2015) attempted to use zircon trace elements distribution to address the issue of distinguishing magmatic and impact related grains using zircon from the investigated here sample 14311. Based on the variation of Th, U and Th/U as well as comparison of zircon REE of a selected set of lunar magmatic rocks and an impact melt, they argued that all grains in the sample younger than 4.3 Ga are of impact origin. Whilst opening a promising new method in the study of lunar zircon this chemistry-based approach cannot unambiguously differentiate between magmatic and impact zircon unless consistent chemical differences are demonstrated for the impact related grains (or parts) identified clearly by means other than their chemical characteristics. This approach should probably include distinction between zircon crystallising from impact melts and those formed by magmatic events and later modified by the impacts as they would possibly have different chemical response to the impact events. The former could be similar to zircon crystallising from the magmas formed by the internal melting of lunar crust and/or mantle. Consequently, relationships between zircon and other minerals in the host rocks as well as zircon internal structures remain the only reliable way to identify zircon grains modified by impacts. Importantly some of the zircon images presented by Hopkins and Mojzsis

(2015) show features that can be attributed to impact related modifications, highlighting the complexity of zircon populations in the impact breccias. No similar internal structures have been identified in the thin sections studied here, though it is important to note that textural relationships of studied zircon grains (Figure 2) suggest that they all are fragments (clasts) in the breccia 14311, even if some of them could have been formed by impacts predating this sample.

Taking into account the difficulties in assigning either magmatic or impact origin to most lunar zircon grains, it is likely that age peaks recorded by the Apollo 14 breccias represent a mixture of material formed by multiple KREEP-magma crystallisation and impact events. Irrespective of the precise interpretation of ages of individual grains in the populations found in Apollo 14 breccias, subtle differences in the age distribution patterns between 14311 and other breccias, in particular the presence of age group centred on 4240 Ma in 14311, which is distinct from the 4200 Ma peak observed in other breccias, suggests a possibility that 14311 has incorporated material from target rocks different from those represented in the majority of the other breccia samples collected at the Apollo 14 landing site. This also raises the possibility that two different impacts were responsible for the formation of these breccias.

This possibility is further supported by the Ca-phosphate ages in impact breccias, which provide constraints on the age of the impact that formed the breccias (Merle et al. 2014; Snape et al. 2016). The age of Ca-phosphates in 14311 (3938 ± 4 Ma, Merle et al. 2014) are older than those in the other breccia samples from the Apollo 14 landing site (combined age for 14305, 14306 and 14314: 3927 ± 2 Ma, Snape et al. 2016). Both the distinct zircon age distribution patterns and the Ca-phosphate ages imply that 14311 sampled different target rocks and formed before the other Apollo 14 breccias during an impact different from that responsible for the formation of most of the other Apollo 14 breccias.

The fate of breccia sample 14311

To determine the origin of 14311 and the mechanism of its delivery to the Apollo 14 landing site several pieces of information need to be taken into account:

1. The presence of a significant number of zircon grains and fragments (>100) in the sample suggests that its source is likely located within the Procellarum KREEP terrane (PKT). Indeed, the PKT is characterised by a high content of incompatible elements (Jolliff et al. 2000), including zirconium as required for the formation of zircons (Dickinson and Hess 1982). While there are a few smaller domains on the Moon showing similar enrichment including the South Pole-Aitken basin, the proximity of the Apollo 14 landing site to PKT has resulted in the interpretation of observed enrichment in elements such as Th in impact melt breccias from the Apollo 14 and Apollo 12 landing sites (Korotev et al. 2011) as an indication of their origin in the PKT.
2. Assuming that the Ca-phosphate ages in the majority of breccia samples from Apollo 14 landing site date the Imbrium impact at 3927 ± 2 Ma (Snape et al. 2016), the Ca-phosphate age of 14311 at 3938 ± 4 Ma (Merle et al. 2014) predates formation of the Imbrium basin by about 10 Ma.

3. Zircon radiation damage was annealed at about 3400 Ma (Pidgeon et al. 2016), indicating a temperature spike at this time in excess of ~230 °C well below the U-Pb system closure temperature of the Ca-phosphates (450–500 °C; Cherniak et al. 1991; Krogstad and Walker 1994; Chamberlain and Bowring 2000). To explain this increase of temperature Pidgeon et al. (2016) suggested that the 14311 breccia may have resided in the vicinity of hot basaltic flows, capable of providing a long-lasting temperature perturbation to the sample and consequent annealing of the radiation damage in zircon grains. Since this age is the only annealing age available for the Apollo 14 breccias, it is still uncertain whether this thermal event affected the Apollo 14 landing site or sample 14311 only.

4. The pre-Cone Crater exposure age of 14311 is 550-660 Ma (Drodz et al. 1974; Stadermann et al. 1991). The exposure age is a cumulative feature that reflects a total residence of the sample on the lunar surface since its formation. The ~600 Ma exposure age reflects the time 14311 spent on the lunar surface and in the simplest scenario, it reflects the time when the sample was finally delivered to the Apollo 14 landing site. In a complex scenario, it represents the sum of different periods of time this sample spent at the surface of the Moon. However, the event at 3400 Ma that resulted in the heating of the sample and recovery of zircon lattice (Pidgeon et al. 2016) could also have outgassed the sample, resetting the noble gas system and exposure age.

Considering these constraints, two scenarios are possible:

1) Breccia 14311 was formed somewhere in the Procellarum KREEP terrane by a 3938 Ma impact. It was deposited on either the Apollo 14 landing site or near the future site of the Imbrium basin by the ejecta of this impact. At ca. 3927 Ma, it was integrated into the Fra Mauro Formation during the deposition of the Imbrium impact ejecta. The zircons were annealed during mare basalt flow extrusion at ca. 3400 Ma at the Apollo 14 landing site. A small and local impact event excavated this sample at approximately 600 Ma and it has been at the surface of the Moon since.

2) Breccia 14311 was formed by the 3938 Ma impact event but was not transported by the Imbrium impact to the Apollo 14 landing site and never incorporated into the Fra Mauro Formation. It was transported from its deposition location to the Apollo 14 landing site by an impact at approximately 600 Ma and remained on the surface of the Moon since this event. In such a hypothesis, the breccia proximal to, or buried by, hot basaltic flows at 3400 Ma, before it was transported to the Apollo 14 landing site.

An alternative explanation for the temperature increase associated with the zircon annealing is an impact postdating breccia formation. However, the temperature spike related to an impact is probably too short to allow the recovery of damaged zircon lattice and residence in a hot ejecta blanket is required to provide sufficient time to make zircon crystalline again at 3400 Ma. If the mare basalt extrusion was not the cause of the 3400 Ma thermal event but rather an impact, a third scenario has to be considered. In this scenario, the 14311 breccia was formed by the 3938 Ma impact and resided on the surface of the Moon for approximately 540 m.y. At 3400 Ma, the sample was transported to the Apollo 14 landing site by an impact, ejecta from whichmay or may not have been mixed with Fra Mauro Formation. Sample 14311 was then buried, hence stopping the cosmic-ray noble gas clocks. The sample was eventually excavated by the Cone Crater impact at 30 Ma leading to a final cumulative exposure age of approximately 600 Ma.

In the case where 14311 was local to the Apollo 14 landing site prior to the 3400 Ma event (hypothesis 1), and where the annealing of the zircons at 3400 Ma was caused by the breccia being included within an ejecta blanket covering the landing site (hypothesis 3), evidence of the 3400 Ma event should also be expected in other Apollo 14 samples. Therefore, identification of the 3400 Ma annealing age in other Apollo 14 zircons would be a reliable test for those hypotheses. The lack of such an age in other samples would imply that hypothesis 2 is the more likely explanation.

The hypothesis suggesting that sample 14311 is exotic to the Apollo 14 landing site and was transported at this location by a ~600 Ma old impact (hypothesis 2) seems to be the simplest scenario. Considering the present data, it is difficult to identify with confidence the crater formed by this impact. A possible candidate is the impact that formed the Copernicus crater, for the following reasons:

1) It is located only 360 km to the north of the Apollo 14 landing site and bright ray of material associated with the Copernicus crater covers much of the Apollo 14 landing site area (e.g. Chapman et al. 1971).

2) The accepted age for the Copernicus crater is between 800 ± 15 Ma (Stöffler et al. 2006) and 779 Ma ± 120 Ma (Hiesinger et al. 2012). Considering their uncertainties, these ages overlap with the estimated exposure age of 550-660 Ma for sample 14311.

3) Basalts in the area around the Copernicus crater (southern Imbrium basalt flows) have an age around 3450 ± 50 Ma (Hiesinger et al. 2000), which is in agreement with a 3400 Ma thermal event recorded by the zircon annealing age.

The main argument against this crater is the thickness of the Imbrium ejecta in the location of the Copernicus crater that could preclude the thermal annealing of the zircons. Indeed, the Copernicus crater is located approximately 800 km away from the centre of the Imbrium basin. Therefore, the site of the Copernicus impact was likely covered by Imbrium ejecta, potentially as thick as 1000 m (McGretchin et al. 1973). According to numerical modelling of heat transfer from lava flows to the underlying regolith, a temperature higher than 300°C is never reached below (i) 20 cm within the regolith when it is overlain by a 1m-thick lava flow or (ii) 2-3 m where the lava flow is 10m thick (Rumpf et al. 2013; Fagents et al. 2010). In the case of sample 14311 buried deep within or underneath the Imbium ejecta, such a thick deposit could have acted as an insulation blanket against the heat provided by the 3400 Ma basaltic flows hence precluding the annealing of the zircons.

Since the thickness of the Imbrium ejecta at the Copernicus site is not well known, however, and we have no constraints for the position of sample 14311 within the Fra Mauro Formation, the hypothesis of 14311 being excavated by the Copernicus impact and transported to the Apollo 14 landing site by its ejecta remains plausible.

The Kepler impact event could be also a possible candidate for the transportation of sample 14311 to the site of Apollo 14 landing site as it is located approximately 400 km from this landing site. The age of this impact, which postdates the formation of Copernicus is not precisely known but has been estimated at 625-1250 Ma (König et al, 1977). The age of the mare basalts in the immediate vicinity of the Kepler crater is also not well constrained with estimates ranging between 3600 and 3100 Ma (Hiesinger et al., 2003). In addition, no deposits of this impact have been found at the Apollo 14 landing site.

CONCLUSIONS

Breccia sample 14311 differs in several ways from other breccias at the Apollo 14 landing site. In particular, its distinct zircon age pattern suggests that it formed from target rocks different from those that formed the other Apollo 14 breccias. Considering that only rocks from the KREEP-rich Procellarum Terrane are known to contain zircon, the target rocks likely originated from this region of the Moon. Since the formation of sample 14311 predates by 10 m.y. the formation of the other Apollo 14 breccias during the Imbrium impact, 14311 might be foreign to the Apollo 14 landing site. This breccia could have been transported to the landing site long after it was formed by a pre-Imbrium impact. The simplest scenario is the formation of this breccia during an impact at 3938 Ma followed by transportation to the Apollo 14 location by a ~600 Ma old impact possibly the event that formed the Copernicus crater.

Acknowledgements

We thank the crew of the Apollo14 spacecraft for carrying back to Earth invaluable samples. The U-Pb work was partly made at the NordSIMS facility that is operated under a joint Nordic agreement. The SEM imaging and EDS data and the SHRIMP work were made with the technical support of the John De Laeter Centre. This work was funded by the Australian Research Council Discovery Project DP120102457 and grants from the Swedish Research Council (VR 621-2012-4370) and the Knut and Alice Wallenberg Foundation (2012.0097).

REFERENCES

Cameron K. L. and Fischer G. W. 1975. Olivine-matrix reactions in thermally metamorphosed Apollo 14 breccias. *Earth Planetary Sciences Letters* 25: 197-207.

Carlson I. C. and Walton W. J. A. 1978. Apollo 14 rock samples. Johnson Space Center Publication #14240, Houston, Texas.

Cavosie A. J., Erickson, T. M., Timms N. E., Reddy S. M., Talavera C., Montalvo S. D., Pincus M. R., Gibbon R. J. and Moser D. 2015. A terrestrial perspective on using ex situ shocked zircons to date lunar impacts. *Geology*: 43, 999-1002.

Chamberlain K. R. and Bowring S. A. 2000. Apatite-feldspar U-Pb thermochronometer: A reliable, mid-range (~450 °C), diffusion controlled system. *Chemical Geology* 172: 73-200.

Chapman P. K., Calio A. J. and Simmons M. G. 1971. Summary of scientific results. *Apollo 14: Preliminary Science Report*. Scientific and Technical Information Office, National Aeronautics and Space Administration, 1-8.

Cherniak D. J., Lanford W. A., and Ryerson F. J. 1991. Lead diffusion in apatite and zircon using ion implantation and Rutherford backscattering techniques. *Geochimica et Cosmochimica Acta* 55: 1663-1673.

Compston W., Williams I. S., and Meyer C. 1984. U-Pb, geochronology of zircons from lunar breccia 73217, using a sensitive high mass-resolution ion microprobe. Proceedings, 14th Lunar and Planetary Science Conference, Part 2. *Journal of Geophysical Research* 89 (supplement): 525-534.

Crozaz G., Drozd R., Hohenberg C. M., Hoyt H. P., Ragan D., Walker R. M. and Yuhas D. 1972. Solar hare and galactic cosmic ray studies of Apollo 14 and 15 samples. Proceedings, 3rd Lunar Science Conference, *Geochimica et Cosmochimica Acta* 3 (Supplement): 2917-2931.

Dalrymple G. B. and Ryder G. 1993. ^{40}Ar/^{39}Ar age spectra of Apollo 15 impact melt rocks by laser step-heating and their bearing on the history of the lunar basin formation. *Journal of Geophysical Research* 98: 13085-13095.

Deutsch A. and Stöffler D. 1987. Rb-Sr-analyses of Apollo 16 melt rocks and a new age estimate for the Imbrium basin: Lunar basin chronology and the early heavy bombardment of the moon. *Geochimica et Cosmochimica Acta* 51: 951-1964.

Dickinson J. E. and Hess P. C. 1982. Zircon saturation in lunar basalts and granites. *Earth Planetary Sciences Letters* 57: 336-344.

Drozd R. J., Hohenberg C. M., Morgan C. J. and Ralston C. E. 1974. Cosmic-ray exposure history at the Apollo 16 and other lunar sites: lunar surface dynamics. *Geochimica et Cosmochimica Acta* 38: 1625-1642.

Eggleton R. E. and Offield T. W. 1970. Geologic Maps of the Fra Mauro region of the Moon, U.S. Geological Survey Misc. Geo. Inv. Map 1-708

Eugster O., Eberhardt P., Geiss J., Grögler N., Jungck, M., Meier F., Mörgell M. and Niederer F. 1984. Cosmic ray exposure histories of Apollo 14, Apollo 15, and Apollo 16 rocks. Proceedings of the 14th Lunar and Planetary Science Conference, *Journal of Geophysical Research*: 89 (Supplement), B498-B512.

Fagents S. A., Rumpf M. E., Crawford I. A. and Joy K. H. 2010. Preservation potential of implanted solar wind volatiles in lunar paleoregolith deposits buried by lava flows. *Icarus* 207: 595-604.

Fedo, C. M., Sircombe, K. N. and Rainbird R. H. 2003. Detrital zircon analysis of the sedimentary record. *Reviews in Mineralogy and Geochemistry* 53.

Gehrels G.E. 2000. Introduction to detrital zircon studies of Paleozoic and Triassic strata in western Nevada and northern California. *Special Paper of the Geological Society of America* 347: 1-17.

Gnos E., Hofmann B. A., Al-Katgiri A., Lorenzetti S., Eugster O., Whitehouse M. J., Villa I. M., Jull A. J. T., Eikenberg J., Spettel, B., Krähenbühl U., Franchi I. A. and Greenwood R. C. 2004. Pinpointing the source of a lunar meteorite: Implications for the evolution of the Moon. *Science* 305: 657–659.

Grange M. L., Pidgeon R. T., Nemchin A. A., Timms N. E., Meyer, C. 2013. Interpreting U-Pb data from primary and secondary features in lunar zircon *Geochimica et Cosmochimica Acta* 101: 112-132.

Haskin L. A., Korotev R. L., Gillis J. J. and Jolliff B. L. 2002. Stratigraphies of Apollo and Luna highland landing sites and provenances of materials from the perspective of basin impact ejecta modeling. Proceedings, *33rd Lunar and Planetary Science Conference*, #1364.

Hawke B. R. and Head J.W. 1978. Lunar KREEP volcanism: geologic evidence for history and mode of emplacement. Proceedings, *9th Lunar and Planetary Science Conference*, pp. 3285-3309.

Hiesinger H., Jaumann, R., Neukum, G. and Head III, J. W. 2000. Ages of mare basalts on the lunar nearside. *Journal of Geophysical Research E: Planets* 105: 29239-29275.

Hiesinger H., Head J. W. III, Wolf U., Jaumann R. and Neukum G. 2003. Ages and stratigraphy of mare basalts in Oceanus Procellarum, Mare Nubium, Mare Cognitum, and Mare Insularum. *Journal of Geophysical Research* 108: doi:10.1029/2002JE001985.

Hiesinger H., Van Der Bogert C. H., Pasckert J. H., Funcke L., Giacomini L., Ostrach L. R. and Robinson M. S. 2012. How old are young lunar craters? *Journal of Geophysical Research E: Planets* 117: E00H10.

Hopkins M. D. and Mojzsis S. J. 2015. A protracted timeline for lunar bombardment from mineral chemistry, Ti thermometry and U–Pb geochronology of Apollo 14 melt breccia zircons. *Contributions to Mineralogy and Petrology* 169: 18 DOI 10.1007/s00410-015-1123-x.

Jolliff B. L., Korotev R .L. and Haskin L. A. 1991. Geochemistry of 2-4-mm particles from Apollo 14 Soil (14161) and implications regarding igneous components and soil-forming processes. Proceedings, *21th Lunar and Planetary Science Conference*. 193-219.

Jolliff B. L., Gillis J. J., Haskin L. A., Korotev, R. L. and Wieczorek, M. A. 2000. Major lunar crustal terranes: Surface expressions and crust-mantle origins, *Journal of Geophysical Research E: Planets*: 105, 4197-4216.

König B., Neukum G., and Fechtig H. 1977. Recent lunar cratering: absolute ages of Kepler, Aristarchus, Tycho (abstract). *Lunar Sci. VIII,* 555-557.

Korotev R. L., Jolliff B. L., Zeigler R. A., Seddio S. M. and Haskin L. A. 2011. Apollo 12 revisited. *Geochimica et Cosmochimica Acta* 75: 1540-1573.

Kovach R. L., Watkins J. S., and Landers T. 1971. Active seismic experiment, Apollo 14 Preliminary Science Report NASA Spec. Paper SP-272, 163.

Krogstad E. J. and Walker R. J. 1994. Higher closure temperatures of the U-Pb system in large apatites from the Tin Mountain pegmatite, Black Hills, South Dakota, USA. *Geochimica et Cosmochimica Acta* 58: 3845-3853.

Liu D., Jolliff B. L., Zeigler R. A., Korotev R. L., Yushan Wan Y., Xie H., Yuhai Zhang, Dong C. and Wang W. 2012. Comparative zircon U–Pb geochronology of impact melt breccias from Apollo 12 and lunar meteorite SaU 169, and implications for the age of the Imbrium impact. *Earth and Planetary Sciences letters* 319-320: 277-286.

Ludwig K. R. 2008. User’s Manual for Isoplot 3.60, A geochronological toolkit for Microsoft Excel. Berkeley Geochronological Center Special Publication no 4, revision of 8 April 2008, 77 pp.

Ludwig K. R. 2009. Squid 2 – A User’s manual (rev 2.50). Berkeley Geochronology Center, Special Publication, 100pp.

McGetchin, T.R., Settle M. and Head J.W. 1973. Radial thickness variation in impact crater ejecta: implications for lunar basin deposits. *Earth and Planetary Sciences letters* 20: 226-236.

Merle R., Nemchin A., Grange M., Whitehouse M. and Pidgeon R. T. 2014. High-resolution U-Pb Ca-phosphate ages in Apollo 14 breccias: implications for the age of the Imbrium impact. *Meteoritics and Planetary science* 49: 2241-2251,

Meyer C., Williams I. S. and Compston W. (1996). Uranium-lead ages for lunar zircons: Evidence for a prolonged period of granophyre formation from 4.32 to 3.88 Ga. *Meteoritics and Planetary Science* 31: 370-387.

Meyer C. 2008. Lunar sample Compendium 14311. http://curator.jsc.nasa.gov/lunar/lsc/14311.pdf.

Morrison R. H. and Oberbeck V. R. 1975. Geomorphology ofcrater and basin deposits–emplacement of the Fra Mauro formation. Proceedings, *6th Lunar and Planetary Science Conference*, pp. 2503–2530.

Nemchin, A. A., Pidgeon, R. T., Whitehouse, M. J., Vaughan, J. P. and Meyer, C. 2008. SIMS U-Pb study of zircon from Apollo 14 and 17 breccias: Implications for the evolution of lunar KREEP. *Geochimica et Cosmochimica Acta* 72: 668-689.

Pidgeon R. T., Furfaro D., Kennedy A. K., Nemchin A. A. and van Bronswjk W. 1994. Calibration of zircon standards for the Curtin SHRIMP, In 8th Int. Conf. on Geochronology, Cosmochronology and Isotope Geology, Berkeley, U.S. Geological Survey Circular: 1107, 251.

Pidgeon R. T., Nemchin A. A., van Bronswijk W., Geisler T., Meyer C., Compston, W. and Williams, I. S. 2007. Complex history of a zircon aggregate from lunar breccia 73235. *Geochimica et Cosmochimica Acta* 71: 1370-1381.

Pidgeon R. T., Merle R. E., Grange M. L., Nemchin A. A. and Whitehouse M. J. 2016. Annealing of radiation damage in zircons from Apollo 14 impact breccia 14311: Implications for the thermal history of the breccia. *Meteoritics and Planetary Science* 51: 155-166.

Rumpf M. E., Fagents S. A., Crawford I.A. and Joy K.H. 2013. Numerical modeling of lava-regolith heat transfer on the Moon and implications for the preservation of implanted volatiles. *Journal of Geophysical Research E: Planets* 118: 382-397.

Sambridge M. S. and Compston W. 1994. Mixture modelling of multi-component data sets with application to ion-probe zircon ages. *Earth and Planetary Science Letters* 128; 373-390.

Satkoski A. M., Wilkinson B. H., Hietpas J. and Samson S.D. 2013. Likeness among detrital zircon populations-An approach to the comparison of age frequency data in time and space. *Bulletin of the Geological Society of America* 125: 1783-1799.

Schoene B., Crowley J. L., Condon D. J., Schmitz M. D. and Bowring, S. A. 2006. Reassessing the uranium decay constants for geochronology using ID-TIMS U-Pb data. Geochimica et Cosmochimica Acta, 70: 426-445.

Scoon J. H. 1972. Chemical analyses of lunar samples 14003, 14311 and 14321. Proceedings, *3rd Lunar Science Conference*. 1335-1336.

Shih C-Y, Nyquist L. E., Dasch E.J., Bogard D. D., Bansal B. M. and Wiesmann H. 1993. Age of pristine noritic clasts from lunar breccias 15445 and 15455. *Geochimica et Cosmochimica Acta* 57: 915-931.

Simonds C. H., Phinney W. C., Warner J. L., McGee P. E., Geeslin J., Brown R. W. and Rhodes J. M. 1977. Apollo 14 revisited, or breccias aren't so bad after all. Proceedings, 8^{th} *Lunar Science Conference*, 1869-1893.

Sircombe K. N. and Hazelton M. L. 2004. Comparison of detrital zircon age distributions by kernel functional estimation. *Sedimentary Geology* 171: 91-111.

Sircombe K. N. 2000. Quantitative comparison of large sets of geochronological data using multivariate analysis: A provenance study example from Australia. *Geochimica et Cosmochimica Acta* 64: 1593-1616.

Snape J. F., Nemchin, A. A., Grange M. L., Bellucci J. J., Thiessen F. and Whitehouse M. J. 2016. Phosphate ages in Apollo 14 breccias: Resolving multiple impact events with high precision U-Pb SIMS analyses. *Geochimica et Cosmochimica Acta* 174: 13-29.

Stacey J. S. and Kramers J. D. 1975. Approximation of terrestrial lead isotope evolution by a two-stage model. *Earth Planetary Sciences Letters* 26: 207-221.

Stadermann F. J., Heusser E., Jessberger E. K., Lingner S. and Stöffler D. 1991. The case for a younger Imbrium basin: New ^{40}Ar-^{39}Ar ages of Apollo 14 rocks. *Geochimica et Cosmochimica Acta* 55: 2339-2349.

Stöffler D. 1989. Brecciated nature of the Apollo 14 lunar sample suite: A review. Workshop on Moon in Transition: Apollo 14, KREEP, and Evolved Lunar

Rocks (November 14-16, 1988, Houston, Texas, eds. G. J. Taylor and P.H. Warren), Lunar and Planetary Institute Technical report 89-03, 138-144.

Stöffler D., Dence M. R., Graup G. and Abadian M. 1974. Interpretation of ejecta formation at the Apollo 14 and 16 sites by a comparative analysis of experimental, terrestrial, and lunar craters. Proceedings, *5th Lunar and Planetary Science Conference*, pp. 137-150.

Stöffler D., Bobe K. D., Jessberger E. K., Lingner S., Palme H., Spettel B., Stadermann F. and Wänke H. 1989. Fra Mauro Formation, Apollo 14: IV. Synopsis and synthesis of consortium studies. Workshop on Moon in Transition: Apollo 14, KREEP, and Evolved Lunar Rocks (November 14-16, 1988, Houston, Texas, eds. G.J. Taylor and P.H. Warren), Lunar and Planetary Institute Technical report 89-03, 145-148.

Stöffler D., Ryder G., Ivanov B. A., Artemieva N. A., Cintala M. J. and Grieve R. A. F. 2006. Cratering history and lunar chronology. In: Jolliff, B. L., Wieczorek, M. A., Shearer, C. K., Neal, C. R. (Eds.), New Views of the Moon, Reviews in Mineralogy and Geochemistry, Vol. 60. Mineralogical Society of America and Geochemical Society, pp. 519–596.

Swann G. A., Bailey N. G., Batson R. M., Eggleton R. E., Hait M. H., Holt H. E., Larson K. B., Reed V. S., Schaber G. G., Sutton R. L., Trask N. J., Ulrich G. E. and Wilshire H. G. 1977. Geology of the Apollo 14 landing site in the Fra Mauro Highlands. Geological Survey Professional Paper 880, pp 103.

Taylor D. J., McKeegan K. Dand Harrison, T.M. 2009. Lu-Hf zircon evidence for rapid lunar differentiation. *Earth and Planetary Science Letters* 279: 157-164.

Vermeesch P. 2012. On the visualisation of detrital age distributions. *Chemical Geology* 312-313: 190-194.

Vermeesch, P. 2013. Multi-sample comparison of detrital age distributions. *Chemical Geology* 341: 140-146.

Warner J. L. 1972. Metamophism of Apollo 14 breccias. Proceedings, *3rd Lunar and Planetary Science Conference*. pp 623-643.

Wiedenbeck M., Hanchar J. M., Peck W. H., Sylvester P., Valley J., Whitehouse M., Kronz A., Morishita Y., Nasdala L., Fiebig J., Franchi I., Girard J.-P., Greenwood R. C., Hinton R., Kita N., Mason P. R. D., Norman M., Ogasawara M., Piccoli P. M., Rhede D., Satoh H., Schulz-Dobrick B., Skår Ø., Spicuzza M. J., Terada K., Tindle A., Togashi S., Vennemann T., Xie Q. and Zheng Y.-F. 2004. Further characterisation of the 91500 zircon crystal. *Geostandards and Geoanalytical Research* 28: 9-39.

Williams R. J. 1972. The lithification of metamorphism of lunar breccias. *Earth Planetary Sciences Letters* 16: 250-256.

Williams I. S. 1998. U-Th-Pb geochronology by ion microprobe. In Applications of Microanalytical Techniques to Understanding Mineralising Processes, edited by McKibben M. A., Shanks W. C. and Riley W. I., *Reviews in Economic Geology*: 7, 1-35.

Wilshire H. G. and Jackson E. D. 1972. Petrology and stratigraphy of the Fra Mauro formation at the Apollo 14 site. *U.S. Geological Survey Professional Paper:* 785, Washington, DC, pp. 30.

Whitehouse M. J., Kamber B. S. and Moorbath S. 1999. Age significance of U–Th–Pb zircon data from early Archaean rocks of west Greenland—a reassessment based on combined ion microprobe and imaging studies. *Chemical Geology* 160: 201-224.

Whitehouse M. J. and Kamber B. S. 2005. Assigning dates to thin gneissic veins in high-grade metamorphic terranes: a cautionary tale from Akilia, Southwest Greenland. *Journal of Petrology* 46: 291-318.

Figure captions:

Figure 1: (a): Map of Apollo 14 landing site (after Stöffler 1989). The letters refer to the successive stations where samples were collected. The station where the sample investigated in this study was collected is marked by a star and the number of the sample is indicated in bold. The dashed line represents the limit of the continuous Cone crater ejecta blanket. LM = Lunar Module; ALSEP = Apollo Lunar Surface Experiments Package. (b): Locations of Mare Imbrium and Apollo 14 landing site on the near side of the Moon (after Lunar and Planetary Institute web site: http://www.lpi.usra.edu).

Figure 2: Optical (reflected light) images of zircon grains in breccia 14311. (a): Rounded zircon. Sample 14311-4; (b): Angular zircon fragment in sample 14311-7; (c): Subhedral grain yielding the youngest age in sample 14311-8; (d): zircon with radial fractures in the surrounding matrix.

Figure 3: Inverse concordia diagram showing ^{204}Pb-corrected ages obtained in this study from zircons found in the investigated 14311 sample thin sections (14311,4; 14311,5; 14311,7; 14311,8 and 14311,90). Error ellipses are shown at 2 sigma level.

Figure 4: $^{207}Pb/^{206}Pb$ zircon ages distribution plot for the 14311 sample and other breccias from Apollo 14 landing site, based on Kernel Density estimates (KDE) and using the Density plotter algorithm (Vermeesh, 2012). The distribution of the individual analyses of the 14311 and other breccia zircon age datasets is shown as circles below the x-axis of the plot. Data for 14311 are from this study and Hopkins and Mojzsis, 2014. Data for other breccias (14066, 14303, 14304, 14305, 14306 and 14083) are from Nemchin et al. 2008 and Taylor et al. 2009.

Table 1: SIMS U-Pb data of 14311 zircon grains.

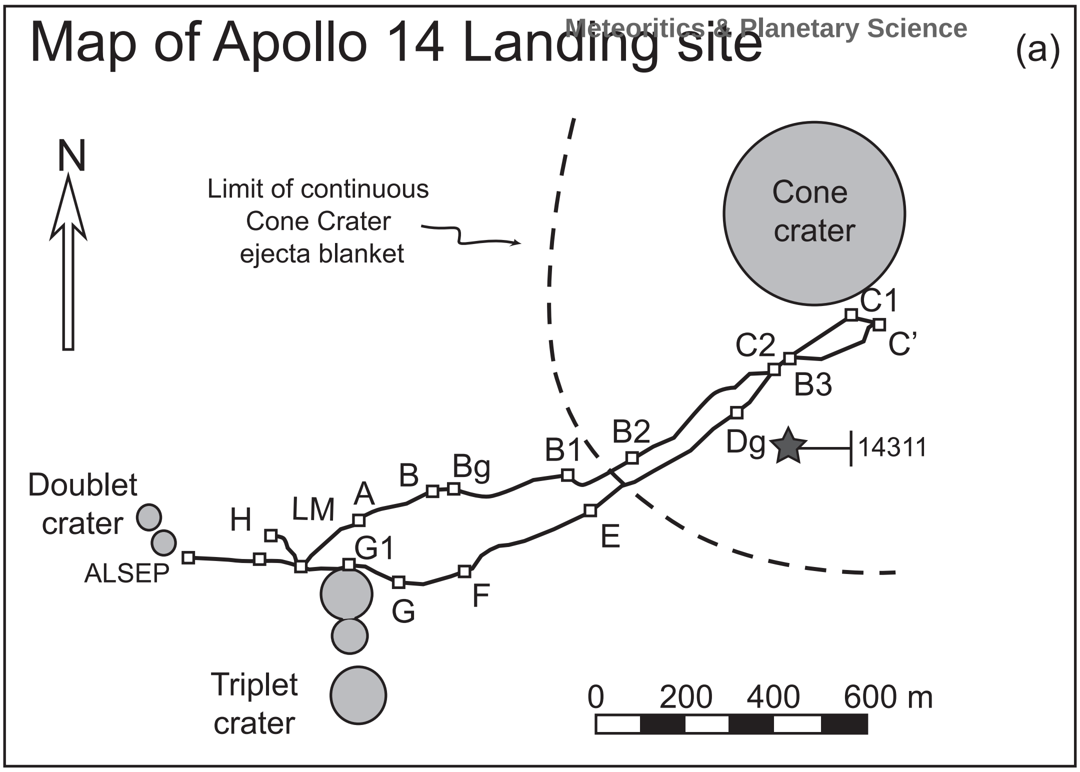
Map of Apollo 14 Landing site
(a)
N
Limit of continuous
Cone Crater
ejecta blanket
Cone
crater
C1
C'
C2
B3
Dg
14311
B2
B1
Bg
B
A
LM
H
Doublet
crater
ALSEP
G1
G
F
E
Triplet
crater
0 200 400 600 m

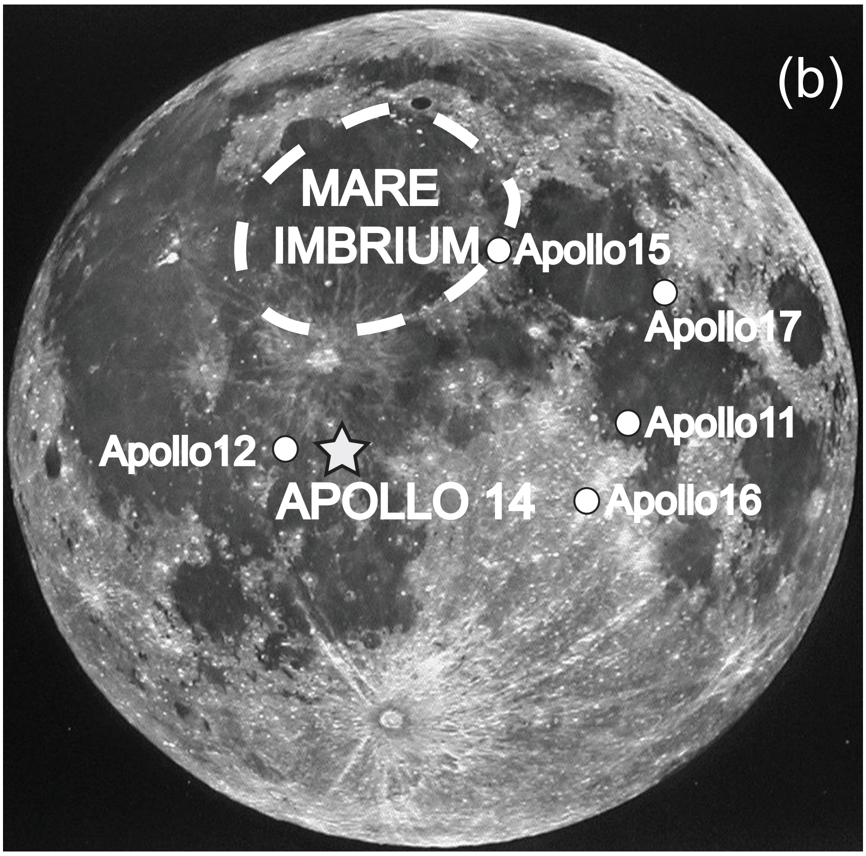
(b)
MARE
IMBRIUM
Apollo15
Apollo17
Apollo11
Apollo12
APOLLO 14
Apollo16

Figure 1

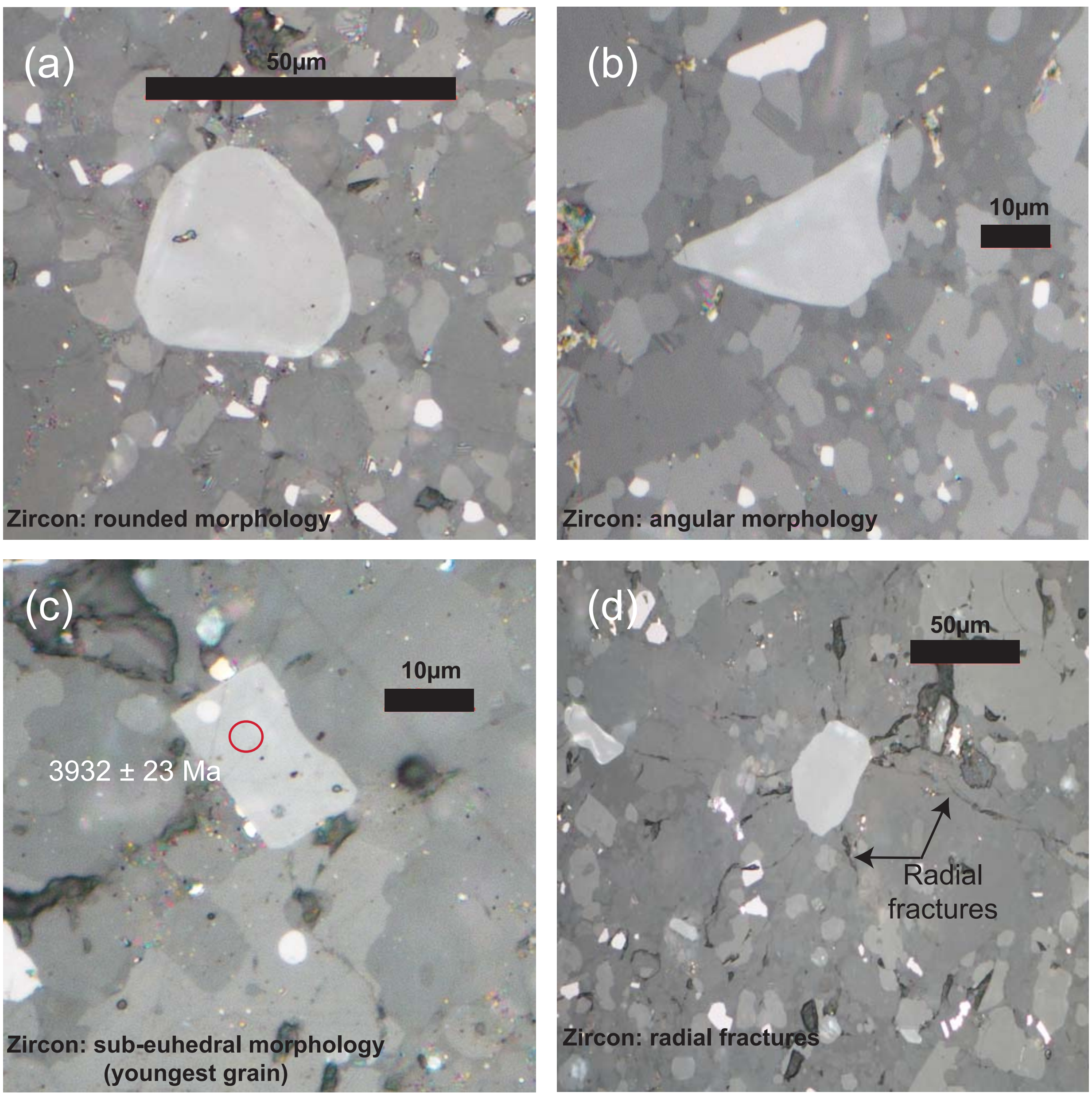
(a)
50μm
Zircon: rounded morphology
(b)
10μm
Zircon: angular morphology
(c)
10μm
3932 ± 23 Ma
Zircon: sub-euhedral morphology
(youngest grain)
(d)
50μm
Radial
fractures
Zircon: radial fractures

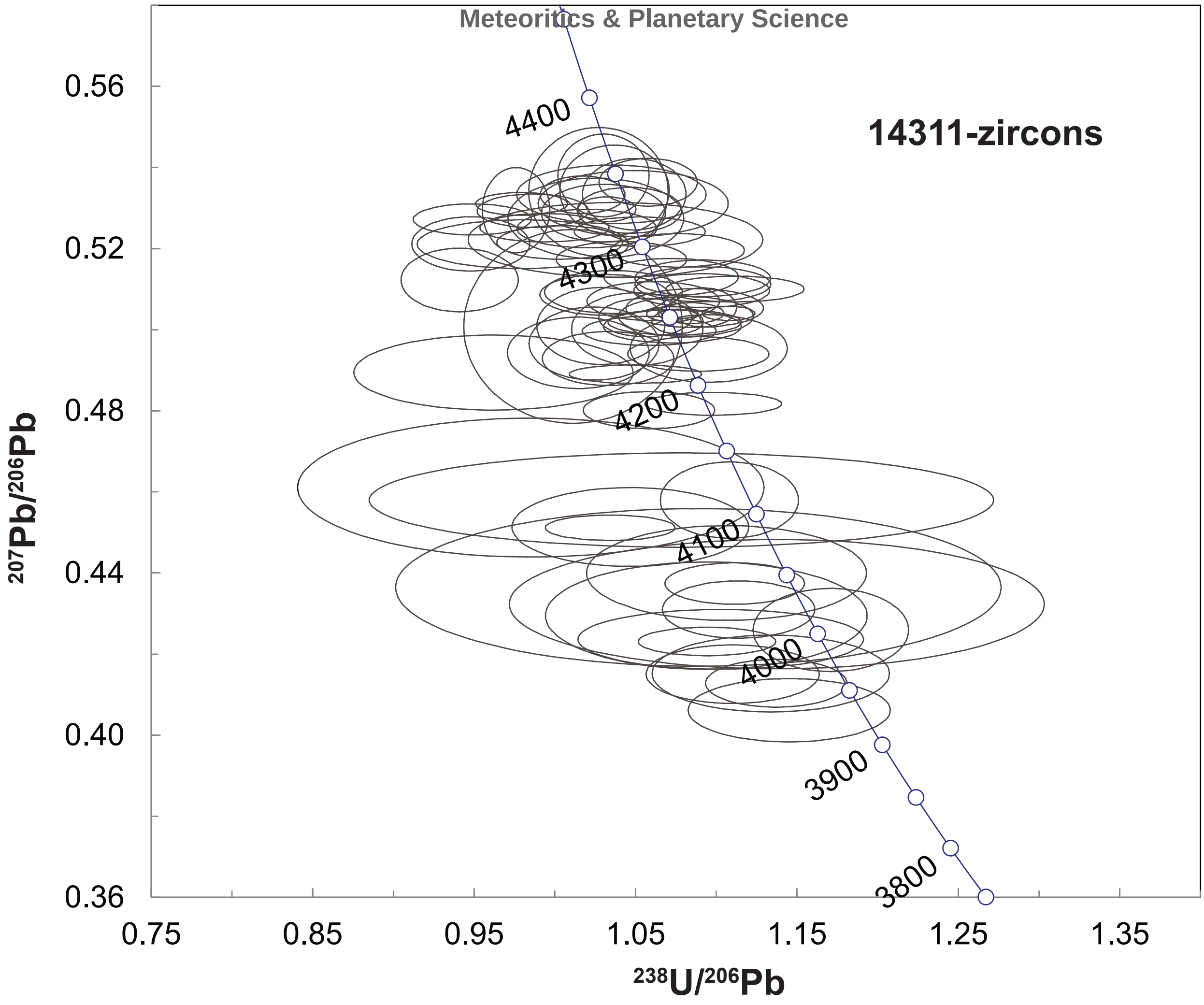
14311-zircons
0.56
0.52
0.48
0.44
0.40
0.36
207Pb/206Pb
0.75
0.85
0.95
1.05
1.15
1.25
1.35
238U/206Pb
4400
4300
4200
4100
4000
3900
3800

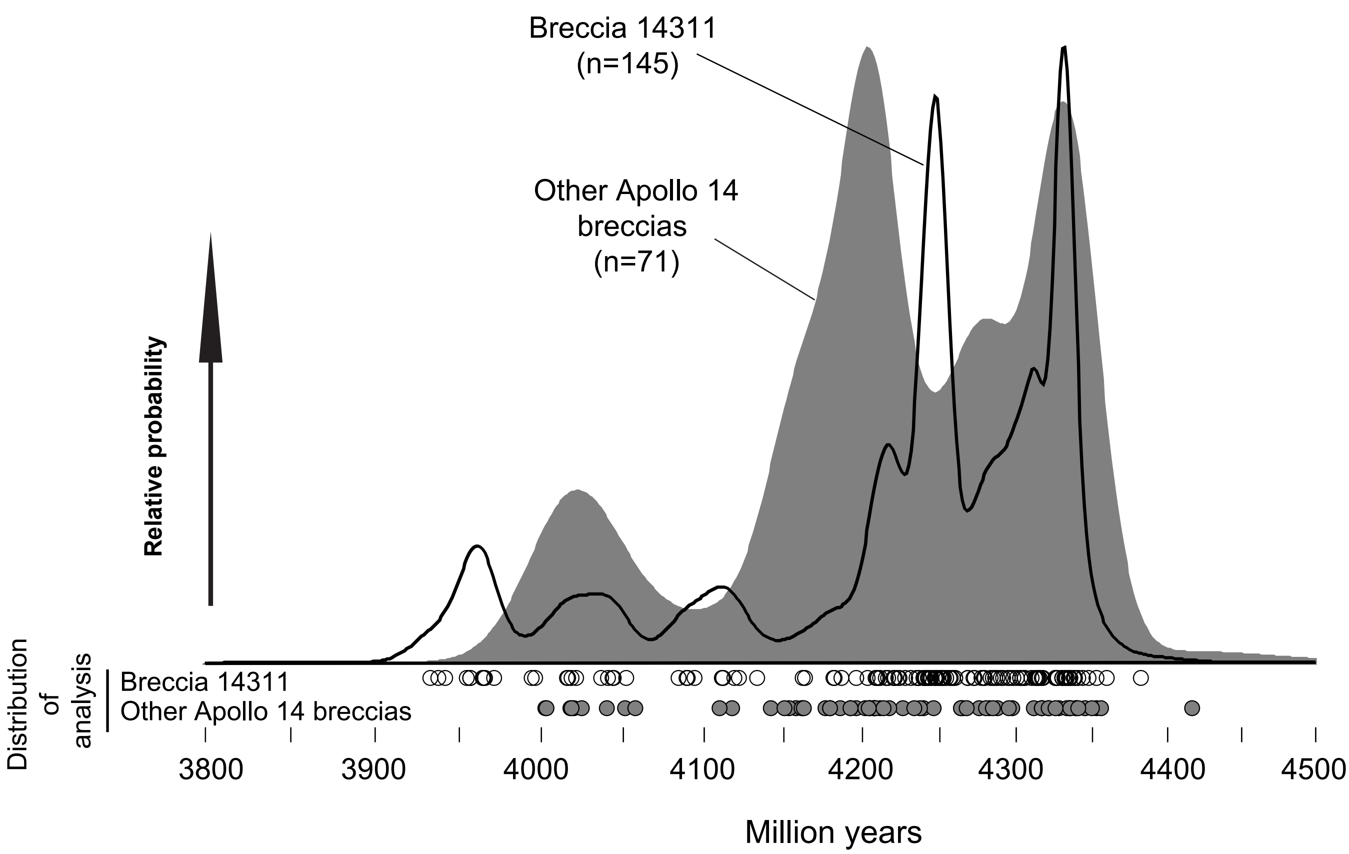
Breccia 14311
(n=145)
Other Apollo 14
breccias
(n=71)
Relative probability
Distribution
of
analysis
Breccia 14311
Other Apollo 14 breccias
3800
3900
4000
4100
4200
4300
4400
4500
Million years

Table 1: U-Pb data obtained on zircon for the East section of Apollo 14 landing site

Sample Name Spot name [a]	**[U] ppm**	**[Th] ppm**	**$^{206}Pb/^{204}Pb$ measured [b]**	**$^{207}Pb^{*}/^{206}Pb^{*}$**	**± 2σ %**	**$^{207}Pb^{*}/^{235}U$**	**± 2σ %**	**$^{206}Pb^{*}/^{238}U$**	**± 2σ %**	**ρ**	**disc. %**
14311,4											
zircon 1											
311-4-zrc1#1	93	56	3762	0.5071	0.78	65.897	3.26	0.9426	3.17	0.97	-1
311-4-zrc1#2	90	52	3753	0.5053	0.77	64.118	3.30	0.9202	3.21	0.97	2
311-4-zrc1#3	82	49	4619	0.5033	0.79	64.180	3.26	0.9249	3.16	0.97	1
zircon 4											
311-4-zrc4	30	11	1102	0.4580	1.68	56.985	3.58	0.9024	3.16	0.88	-1
zircon 7											
14311-4-zrc7	238	107	9549	0.4817	0.48	60.486	3.19	0.9107	3.16	0.99	0
zircon 8											
14311-4-zrc8	55	32	169	0.5222	1.44	69.395	7.34	0.9639	7.19	0.98	-1
zircon 10											
14311-4-zrc10	184	64	4023	0.4374	0.95	54.266	3.32	0.8997	3.18	0.96	-3
zircon 13											
14311-4-zrc13#12	25	12	1152	0.5002	1.46	65.621	3.49	0.9515	3.17	0.91	-2
14311-4-zrc13#13	23	11	1714	0.5009	1.55	67.160	3.51	0.9724	3.15	0.90	-4
14311-4-zrc13#14	23	11	1047	0.4966	1.48	66.854	3.54	0.9764	3.22	0.91	-5
14311-4-zrc13#15	24	12	2488	0.4943	1.46	67.191	3.83	0.9858	3.54	0.93	-6
zircon 14											
14311-4-zrc14#17	97	61	7366	0.5130	0.72	65.984	3.26	0.9328	3.18	0.97	1
14311-4-zrc14#18	93	58	6263	0.5173	0.70	68.508	3.25	0.9605	3.18	0.98	-2
14311,5											
zircon 2											
14311-5-zrc2#1	37	14	8657	0.5030	0.77	65.681	2.37	0.9470	2.24	0.95	-1
14311-5-zrc2#2	42	16	4249	0.5008	0.66	64.365	3.32	0.9321	3.26	0.98	0
zircon 3											
14311-5-zrc3#1	44	19	-	0.5293	0.64	74.006	2.93	1.0140	2.86	0.98	-6
14311-5-zrc3#2	45	19	28507	0.5333	0.71	72.295	2.23	0.9833	2.11	0.95	-2
zircon 4											
14311-5-zrc4	511	253	8663	0.4512	0.57	60.157	3.23	0.9670	3.18	0.98	-9
zircon 5											
14311-5-zrc5#1	90	55	-	0.5310	0.43	74.775	2.42	1.0213	2.38	0.98	-7
zircon 6											
14311-5-zrc6	186	110	11143	0.5251	0.54	72.882	3.34	1.0066	3.29	0.99	-6
zircon 7											
14311-5-zrc7	148	65	28980	0.5215	0.65	71.698	3.24	0.9971	3.18	0.98	-5
zircon 8											
14311-5-zrc8	451	131	1356	0.5212	1.05	75.830	3.32	1.0553	3.15	0.95	-11
zirocn 12											
14311-5-zrc12	31	14	2772	0.4954	1.37	62.359	3.89	0.9130	3.64	0.94	1
zircon 13											
14311-5-zrc13	160	96	44638	0.4997	0.59	65.098	3.26	0.9448	3.20	0.98	-2
zircon 14											
14311-5-zrc14	84	61	2898	0.5123	1.25	75.077	3.40	1.0630	3.16	0.93	-13
zircon 16					0.00						

14311-5-zrc16	78	49	10398	0.4929	1.10	65.797	3.41	0.9681	3.22	0.95	-5
zircon 17											
14311-5-zrc17	119	99	14159	0.4940	0.70	62.560	3.36	0.9184	3.29	0.98	1
zircon 18											
14311-5-zrc18	473	152	48053	0.4891	0.38	64.226	3.22	0.9525	3.20	0.99	-3
14311,7											
zircon 1											
14311-7-zrc1	404	544	823	0.5295	1.62	74.814	2.38	1.0248	1.75	0.73	-7
zircon 2											
14311-7-zrc2	83	53	119	0.5008	3.90	68.293	6.72	0.9890	5.48	0.81	-6
zircon 5											
14311-7-zrc5#1	49	28	166	0.5364	0.90	69.914	2.52	0.9454	2.35	0.93	2
14311-7-zrc5#2	43	21	184	0.5380	1.55	72.026	2.73	0.9709	2.25	0.82	-1
14311-7-zrc5#3	40	19	162	0.5287	1.10	70.779	3.24	0.9709	3.05	0.94	-2
14311-7-zrc5#4	57	31	239	0.5344	1.70	71.062	3.17	0.9644	2.68	0.84	0
14311-7-zrc5#5	53	29	184	0.5334	1.35	70.103	2.84	0.9532	2.50	0.88	1
zircon 6											
14311-7-zrc6	77	43	426	0.5295	0.87	69.779	2.68	0.9559	2.53	0.95	0
zircon 9											
14311-7-zrc9	141	57	646	0.5297	0.47	70.755	1.50	0.9688	1.42	0.95	-1
14311,8											
zircon 1											
14311-8-zrc1	61	33	398	0.4062	1.57	48.903	4.74	0.8732	4.47	0.94	-4
zircon 2											
14311-8-zrc2	64	21	681	0.5340	2.43	71.699	4.21	0.9738	3.44	0.82	-1
zircon 3											
14311-8-zrc3	142	114	281	0.4237	1.42	52.969	6.71	0.9068	6.56	0.98	-6
zircon 4											
14311-8-zrc4	196	103	1086	0.4802	0.78	62.563	3.24	0.9450	3.15	0.97	-4
zircon 11											
14311-8-zrc11	78	49	663	0.4151	1.42	51.552	4.20	0.9008	3.95	0.94	-6
zircon 12											
14311-8-zrc12	116	147	606	0.4310	1.34	53.356	3.72	0.8978	3.47	0.93	-4
zircon 13											
14311-8-zrc13	203	444	223	0.4295	2.52	54.145	7.87	0.9143	7.46	0.95	-6
zircon 15											
14311-8-zrc15	270	93	212	0.4580	2.07	58.559	14.82	0.9273	14.68	0.99	-4
zircon 16											
14311-8-zrc16	137	53	374	0.4152	1.86	50.495	5.62	0.8820	5.30	0.94	-4
zircon 17											
14311-8-zrc17	127	50	291	0.4400	2.16	54.838	6.76	0.9039	6.41	0.95	-3
zircon 18											
14311-8-zrc18	71	41	210	0.4514	1.76	59.456	6.00	0.9553	5.73	0.96	-8
zircon 20											
14311-8-zrc20#12	56	34	600	0.5334	1.11	71.060	4.77	0.9663	4.64	0.97	-1
14311-8-zrc20#14	58	34	615	0.5274	1.54	70.930	4.61	0.9753	4.34	0.94	-2
zircon 21											

14311-8-zrc21#15	299	164	1791	0.5242	0.56	68.671	3.21	0.9501	3.16	0.98	0
14311-8-zrc21#16	333	195	1272	0.5272	0.59	76.622	3.21	1.0541	3.15	0.98	-10
zircon 22											
14311-8-zrc22#17	268	111	1866	0.5096	0.67	64.410	3.23	0.9166	3.16	0.98	2
14311-8-zrc22#18	255	101	2520	0.5127	0.72	64.757	3.23	0.9161	3.15	0.98	3
14311-8-zrc22#19	243	94	2764	0.5100	0.51	63.258	3.19	0.8996	3.15	0.99	4
14311-8-zrc22#20	307	140	580	0.5086	0.81	68.052	3.26	0.9704	3.16	0.97	-3
14311-8-zrc22#21	312	132	1133	0.5093	0.84	67.767	3.47	0.9651	3.36	0.97	-3
14311-8-zrc22#22	250	96	1112	0.5112	0.69	64.561	3.22	0.9160	3.15	0.98	3
zircon 23											
14311-8-zrc23	244	97	489	0.4895	1.54	70.169	7.52	1.0398	7.36	0.98	-13
zircon 24											
14311-8-zrc24	169	100	200	0.4611	3.03	64.545	12.38	1.0153	12.00	0.97	-13
zircon 28											
14311-8-zrc28#28	51	25	159	0.4324	3.01	52.402	12.30	0.8790	11.92	0.97	-1
14311-8-zrc28#29	39	21	588	0.4260	1.96	50.153	3.90	0.8539	3.37	0.86	1
14311-8-zrc28#30	42	22	168	0.4365	3.64	55.268	14.56	0.9184	14.10	0.97	-5
zircon 30											
14311-8-zrc30	134	62	721	0.5249	0.74	70.980	3.55	0.9807	3.47	0.98	-3
zircon 32											
14311-8-zrc32	147	105	631	0.4128	1.16	50.053	3.36	0.8793	3.15	0.94	-4
zircon 33											
14311-8-zrc33	258	112	385	0.5211	0.94	73.308	5.55	1.0203	5.47	0.99	-8
zircon 35											
14311-8-zrc35	137	49	2202	0.5196	0.65	66.582	3.22	0.9294	3.15	0.98	2
zircon 36											
14311-8-zrc36	392	373	586	0.4231	0.68	53.318	3.25	0.9139	3.18	0.98	-7
zircon 37											
14311-8-zrc37	137	90	587	0.5311	1.25	69.848	4.76	0.9538	4.59	0.96	0
zircon 39											
14311-8-zrc39	242	108	1848	0.5018	0.51	64.411	3.19	0.9309	3.15	0.99	0
14311,90											
zircon 1											
311-90-101	240	116	126445	0.5020	0.49	64.333	1.30	0.9294	1.21	0.93	0
311-90-102	251	106	14510	0.5040	0.28	62.746	1.23	0.9029	1.20	0.97	3
311-90-103	256	112	-	0.5041	0.41	64.102	1.59	0.9222	1.54	0.97	1
311-90-104	244	117	20827	0.5055	0.77	63.842	1.74	0.9160	1.56	0.90	2
311-90-105	240	115	4391	0.5039	0.30	64.759	1.26	0.9322	1.22	0.97	0

* indicates radiogenic Pb, i.e. corrected from common Pb (after Stacey and Kramers, 1975)
(a) spot numbers are given only for grains with multiple analyses; spots were numbered sequentially for some samples
(b) (-) indicate that the amount of ^{204}Pb is too small to give a significant ratio

$^{207}Pb/^{206}Pb$ age (Ma)	±2σ (Ma)
4262	11
4257	11
4251	12
4111	25
4186	7
4305	21
4043	14
4242	21
4244	23
4231	22
4224	21
4279	11
4291	10
4250	11
4244	10
4325	9
4336	10
4089	8
4330	6
4313	8
4303	9
4302	15
4228	20
4240	9
4277	18

4220	16
4223	10
4209	6
4325	24
4244	57
4344	13
4349	23
4323	16
4339	25
4336	20
4325	13
4326	7
3932	23
4338	35
3995	21
4181	11
3965	21
4021	20
4016	37
4111	31
3965	28
4052	32
4090	26
4336	16
4320	22

4311	8
4319	9
4269	10
4278	11
4270	7
4266	12
4268	12
4274	10
4210	23
4121	45
4026	45
4003	29
4040	54
4313	11
3957	17
4302	14
4298	10
3993	10
4330	18
4247	8
4247	7
4253	4
4253	6
4257	11
4253	4